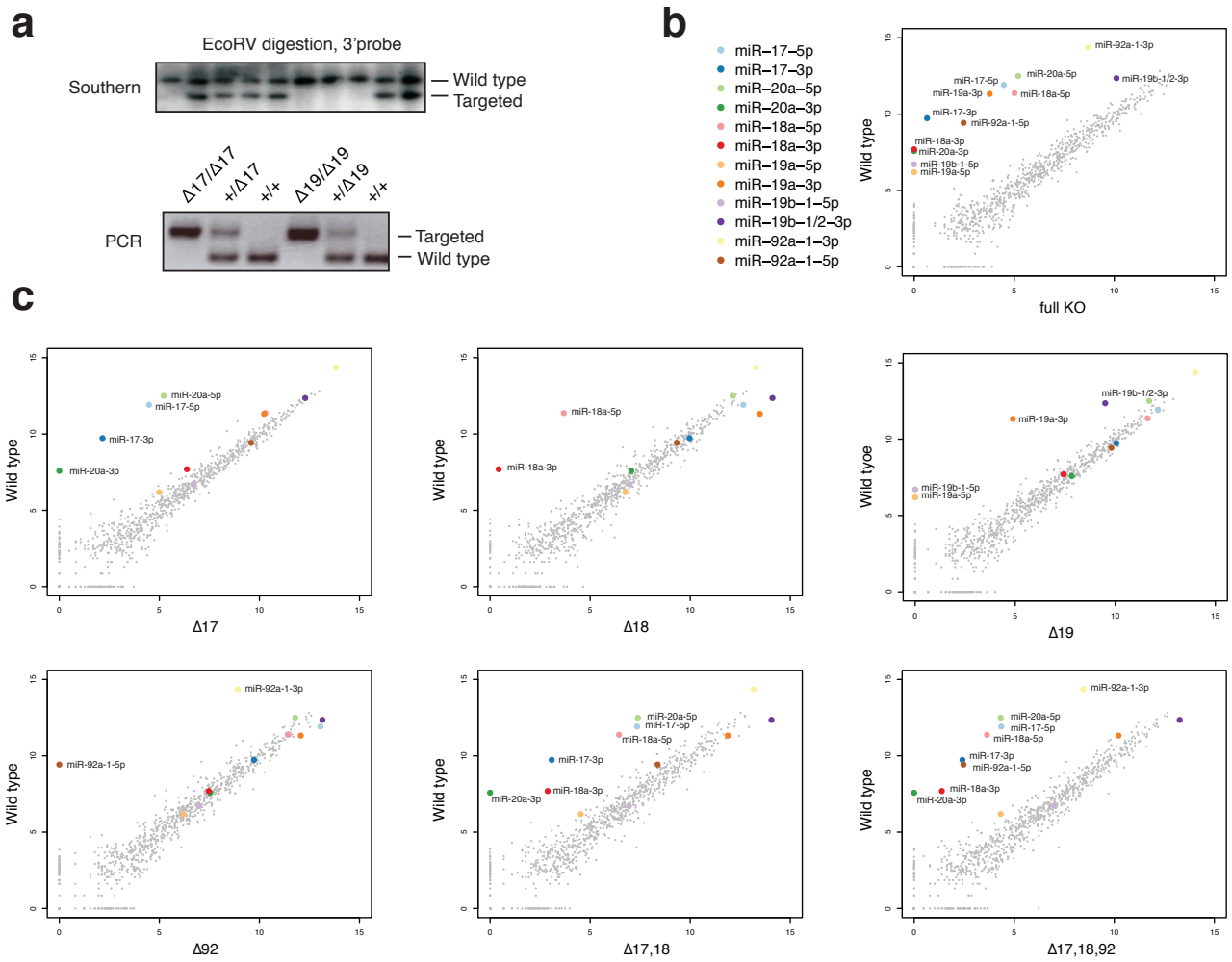


Supplementary Figure 1

***Generation and validation of mice carrying a series of miR-17~92 alleles***

**(a)** *Top*, southern blot to EcoRV-digested genomic DNA extracted from neomycin-selected ES clones targeted with the *miR-17~92*$^{\Delta 17}$ construct; *Bottom*, genotyping PCR showing germline transmission of two *miR-17~92* mutant alleles. **(b,c)** Scatter plots showing miRNA expression as determined by small RNA-seq in *miR-17~92*-null **(b)** or *miR-17~92* allelic series' embryos **(c)** versus a wild type control. Both strands of the miRNAs encoded by the *miR-17~92* cluster are highlighted in color. Expression values are represented as log of normalized counts.

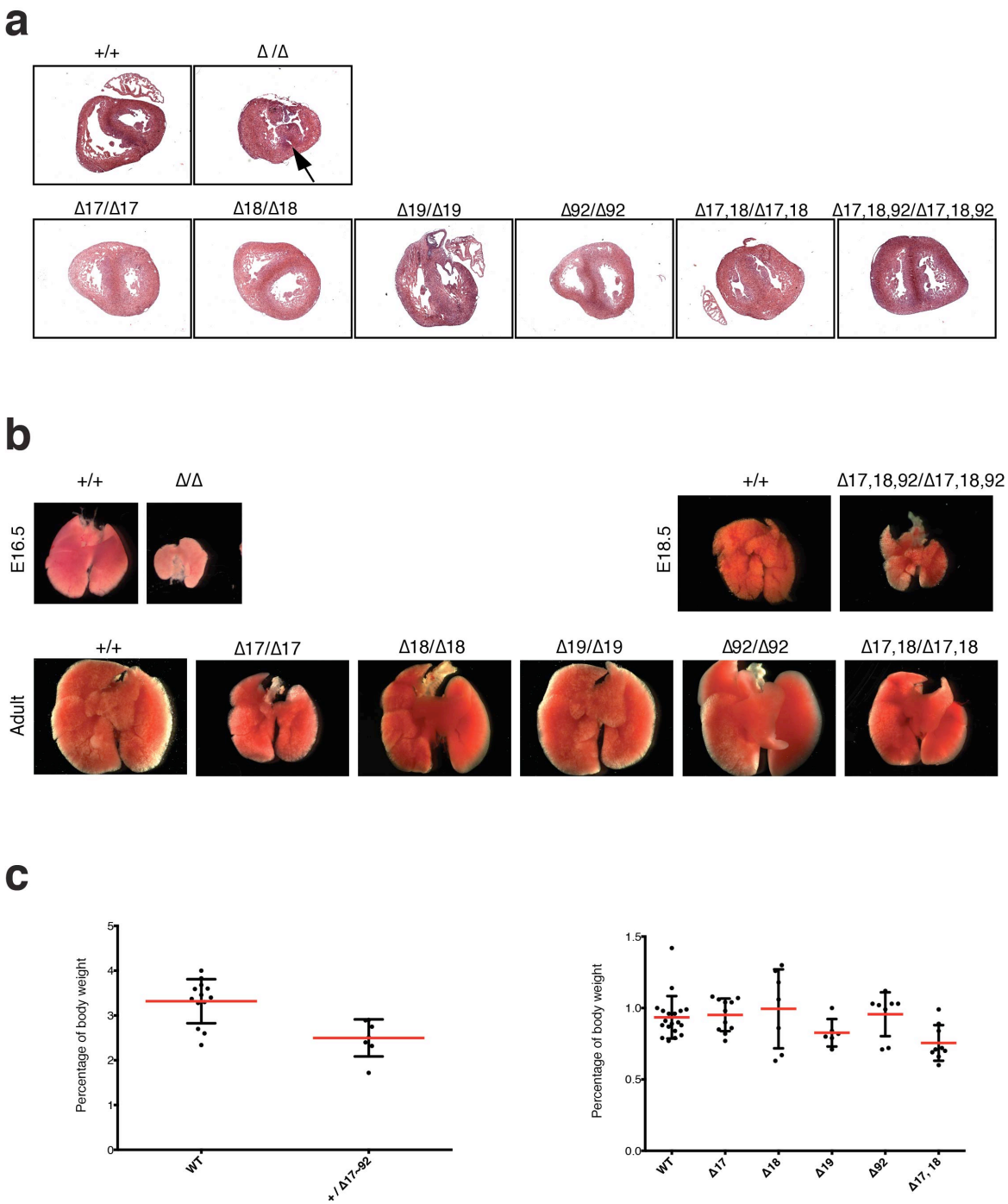


Supplementary Figure 2

***Heart and lung development in miR-17~92 mutant mice***

**(a)** Hematoxylin-eosin stainings of transverse sections of hearts from E18.5 wild type (+/+) *miR-17~92*-null (Δ/Δ) and homozygous embryos from the *miR-17~92* the allelic series. Black arrow indicates a ventricular septal defect (n > 3). **(b)** Macroscopic view of representative lungs from *miR-17~92* mutant animals and wild-type controls. **(c)** Weight of lungs as percentage of total body weight. Red bar represents average. Error bars represent s.d.

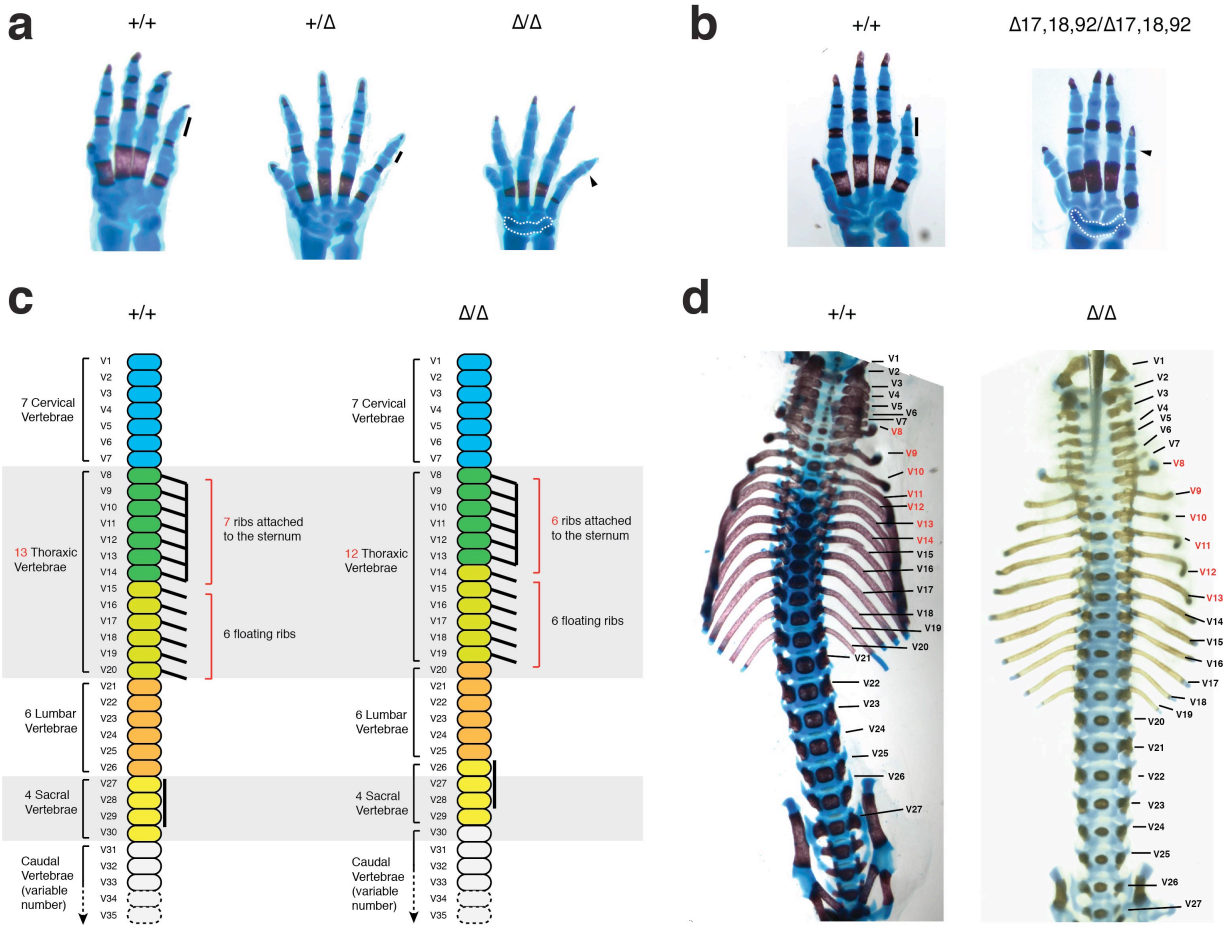


Supplementary Figure 3

***Skeletal defects in miR-179~2 mutant mice***

**(a,b)** Alcian blue/alizarin red stainings of forelimb autopods of *miR-17~92*$^{+/+}$, *miR-17~92*$^{+/\Delta}$ and *miR-17~92*$^{\Delta/\Delta}$ **(a)** or *miR-17~92*$^{+/+}$ and *miR-17~92*$^{\Delta 17,18,92/\Delta 17,18,92}$ E18.5 embryos **(b)**. Black bar represents length of mesophalanx. Arrowhead indicates absence of phalanx. Fusion of carpal bones is indicated by doted line. **(c)** Schematic representation of vertebral patterning in wild type and *miR-17~92*$^{\Delta/\Delta}$ animals. **(d)** Ventral view of the skeletons shown in Fig.3. The position of vertebrae V1 to V27 is indicated. Vertebrae whose ribs attach to the sternum are indicated in red.

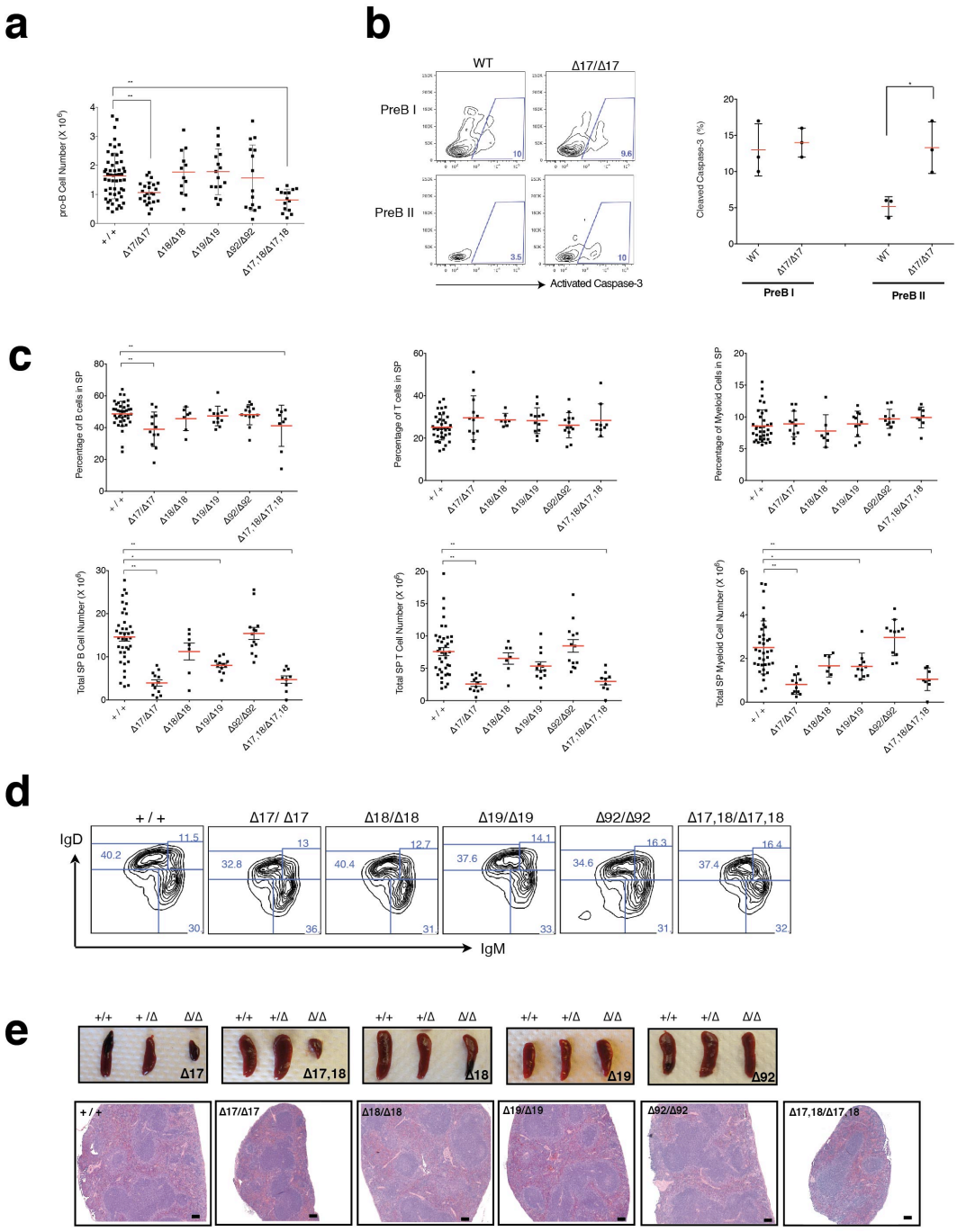


Supplementary Figure 4

***Peripheral Immune system in mice of the miR-17~92 allelic series***

**(a)** Absolute pro-B cell number **(b)** *Left*, representative flow cytometry plots showing the percentage of cleaved caspase-3 positive Pre-BI and Pre-BII cells from 5–7 week-old mice. Results from independent experiments are presented in the *right panel*. **(c)** Relative (*top*) and absolute number (*bottom*) of splenic B cells (B220+), T cells (TCRb+) and myeloid cells (CD11b+) from viable homozygous mutant animals. **(d)** Representative flow cytometry plots of splenic B cells (gated for B220+) showing that the maturation of B cells in all viable mutant mice is comparable to that in wild type controls. **(e)** *Top*, spleens from adult animals. *Bottom,* Hematoxylin and eosin staining of spleen sections from viable homozygous mutant mice at the age of 5–6 weeks showing an intact overall structure of the spleens. Black bar represents 100 $\mu$m. Horizontal red bars indicate the median value for each strain ($n > 8$). * $p < 0.05$, ** $p < 0.001$ (2-tailed t-test).

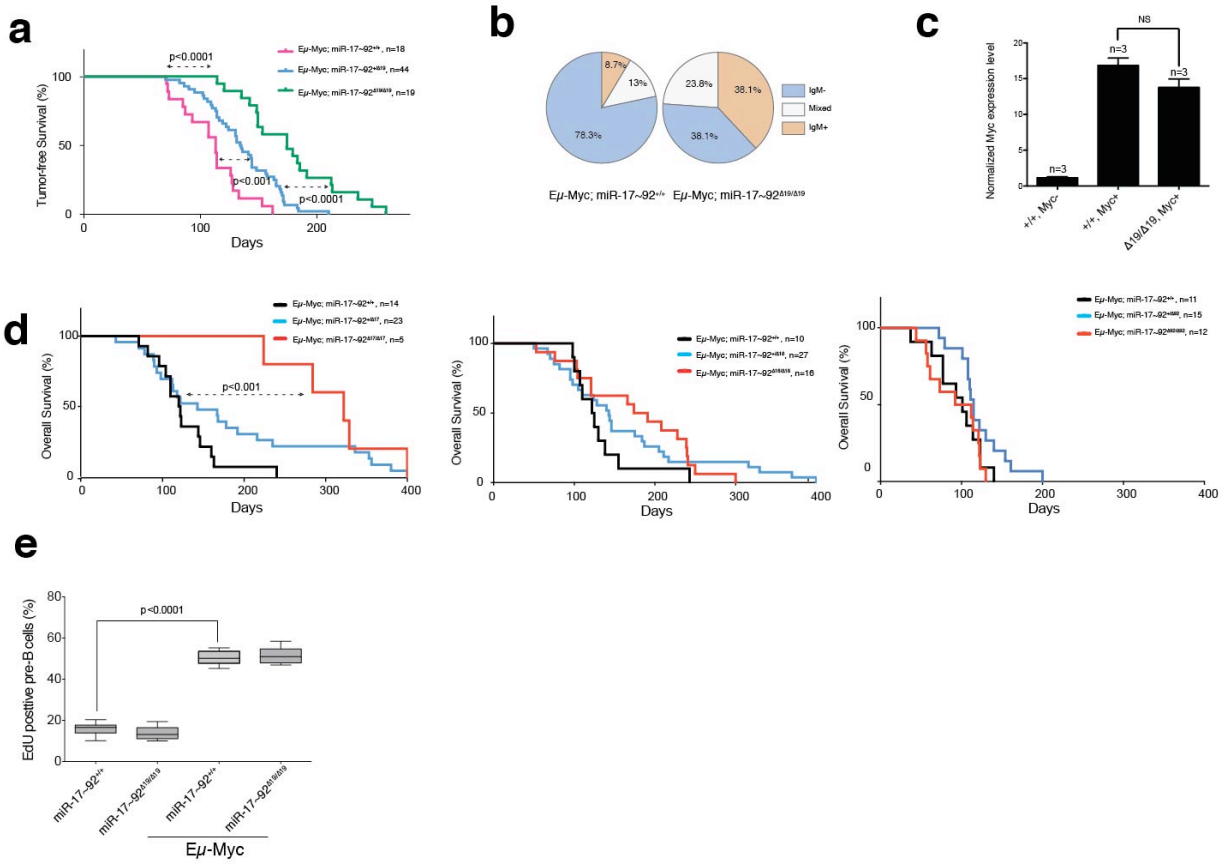


Supplementary Figure 5

***Myc-driven lymphomagenesis in mice from the miR-17~92 allelic series***

**(a)** Tumor free survival curve of *miR-19* deficient mice. **(b)** Immunophenotype of B cell lymphomas (gated for B220+) developing in the spleen of *Eμ-Myc*;*miR-17~92*$^{+/+}$ and *Eμ-Myc*;*miR-17~92*$^{\Delta 19/\Delta 19}$ mice. "Mixed" indicates tumors in which the fraction of IgM+ cells was between 30% and 70%. ($n > 20$ per genotype, $p < 0.0001$; $\chi^2$ test). **(c)** Relative Myc expression in pre-B cells from wild type, *Eμ-Myc;miR-17~92*$^{+/+}$, and *Eμ-Myc;miR-17~92*$^{\Delta 19/\Delta 19}$ animals. **(d)** Survival curve of miR-17, -18 and -92 deficient *Eμ-Myc* mice. p-values, Mantel-Cox test. **(e)** Quantification of the percentage of EdU positive pre-B cells in 5 week-old mice. (p-values, two-tailed t-test).

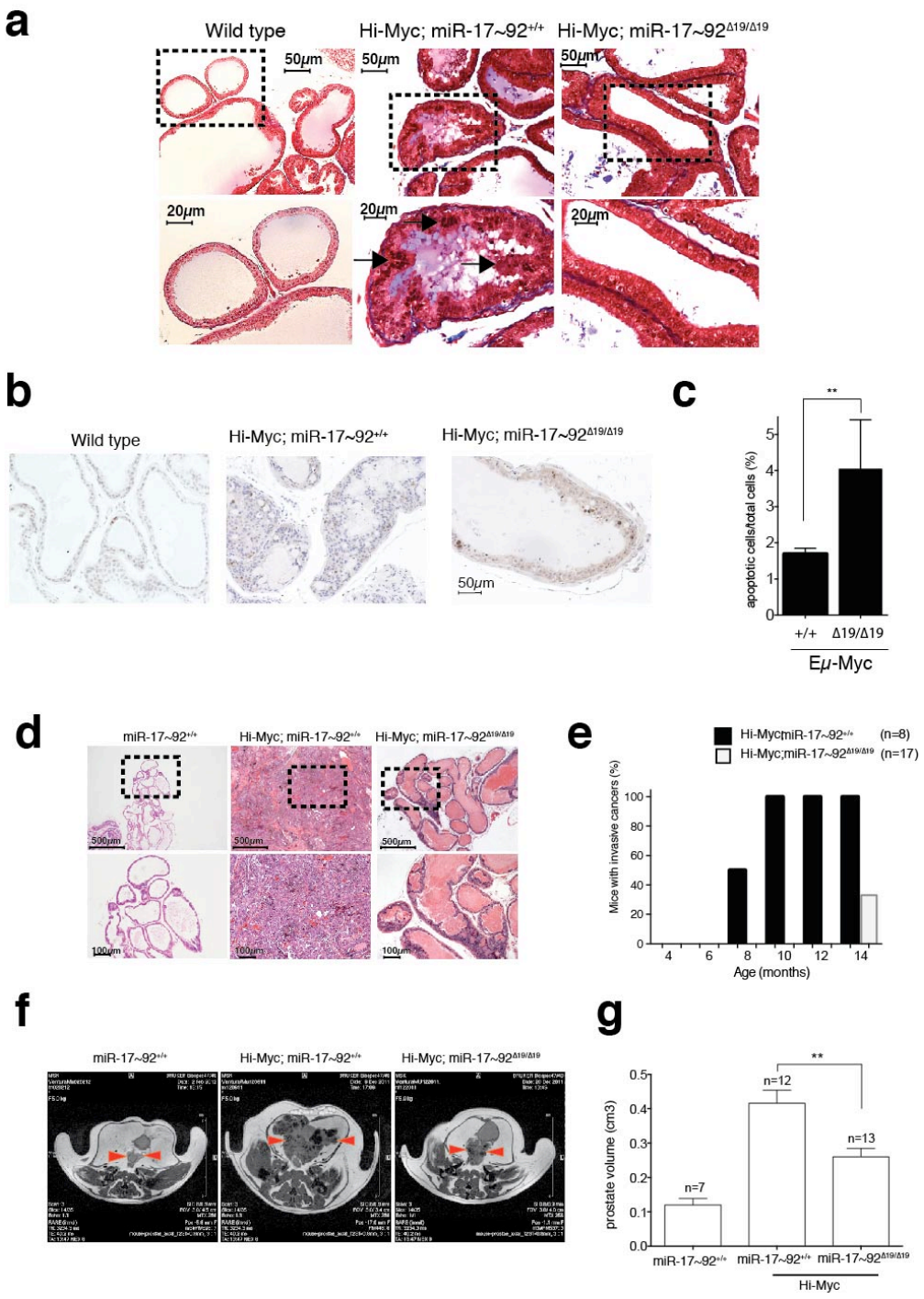


Supplementary Figure 6

***Hi-Myc driven prostate cancer in miR-19-deficient mice***

**(a)** Masson's trichrome staining on prostate sections from 8 week-old mice. Arrows indicate foci of PINs**. (b)** Cleaved caspase-3 immunostaining on prostate sections from 8 week-old mice. **(c)** Bar plot showing the fraction of cleaved caspase-3 cells in E$\mu$-Myc prostates (*miR-17~92*$^{+/+}$ and *miR-17~92*$^{\Delta 19/\Delta 19}$). **(d)** H&E staining on prostate sections from 12 month-old mice. **(e)** Percentage of animals that developed invasive prostate adenocarcinomas up to 14 months of age. **(f)** MRIs showing transverse sections of the pelvic region of 12 month-old mice of the indicated genotypes. Prostates are indicated by red arrows. **(g)** Quantification of prostate volume (2-tailed t-test. Error bars = s.d.).

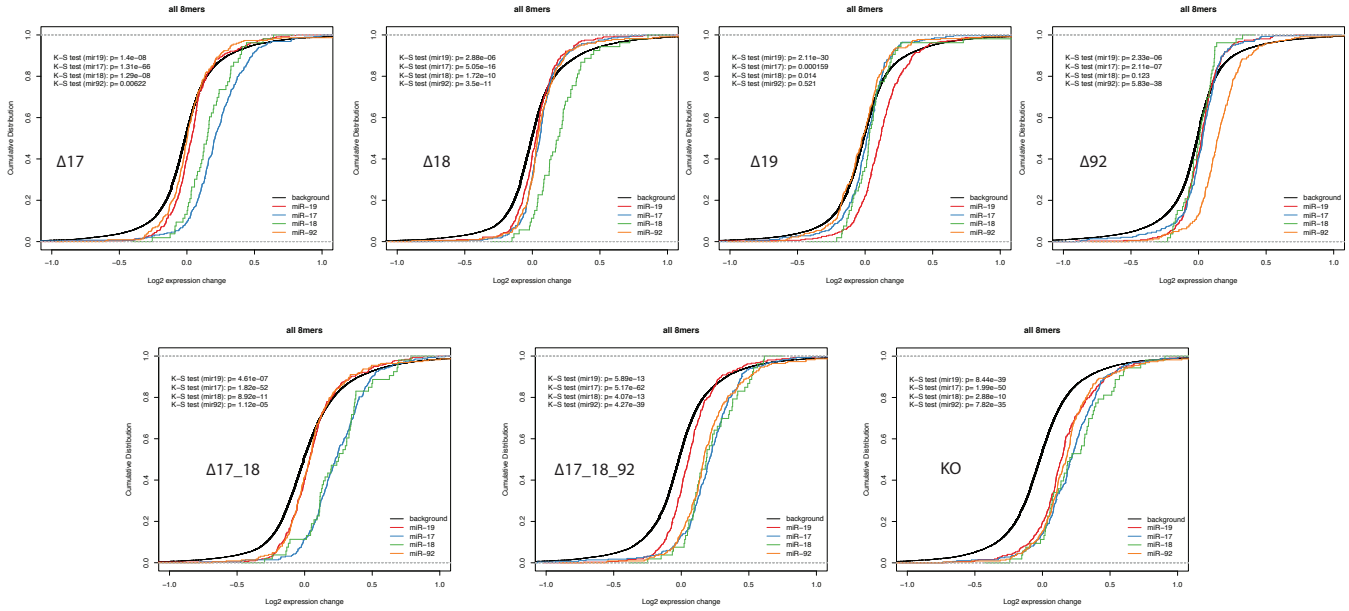


Supplementary Figure 7

**CDF plots of gene expression profiles from the miR-17~92 allelic series.**
Cumulative Distribution Fraction plots of $log_2$-fold changes of genes without (black) or with (colored) 8-mers matches for members of the *miR-17~92* cluster in their 3'UTR. The plots were generated from the tail bud differential expression dataset.

| | WT (25%) | HET (50%) | KO (25%) | Corrected p Value |
|---|---|---|---|---|
| **Δ17** | 50/144 **(35%)** | 84/144 **(58%)** | 10/144 **(7%)** | $1.21 \times 10^{-6}$ |
| **Δ18** | 30/94 **(32%)** | 51/94 **(54%)** | 13/94 **(14%)** | 0.19 |
| **Δ19** | 62/222 **(28%)** | 149/222 **(67%)** | 11/222 **(5%)** | $1.09 \times 10^{-10}$ |
| **Δ92** | 21/84 **(25%)** | 43/84 **(51%)** | 20/84 **(24%)** | 5.79 |
| **Δ17,18** | 37/97 **(38%)** | 57/97 **(59%)** | 3/97 **(3%)** | $9.02 \times 10^{-6}$ |
| **Δ17,18,92** | 27/67 **(40%)** | 40/67 **(60%)** | 0/67 **(0%)** | $3.20 \times 10^{-5}$ |
| **Δ17~92** | 24/60 **(40%)** | 36/60 **(60%)** | 0/60 **(0%)** | $1.42 \times 10^{-4}$ |

Supplementary Table 1.

**Allelic frequencies in C57BL/6J background.**

p-value was calculate using the chi-square test and adjusted for multiple hypothesis testing. Genotypes were determined at postnatal day 10-12.

| | | vertebral fusion | carpal bone fusion | toe syndactyly[a] | cleft palate | ossification delay |
|---|---|---|---|---|---|---|
| miR-17~92 | WT | 0% | 0% | 0% | 0% | 0% |
| | HET | 72% | 0% | 0% | 0% | 0% |
| | KO | 100% | 100% | 100% | 100% | 100% |
| Allelic series | WT | 0% | 0% | 0% | 0% | 0% |
| Δ17 | HET | 17% | 0% | 0% | 0% | 0% |
| | KO | 43% | 25% | 0% | 0% | 100% |
| Δ18 | HET | 0% | 0% | 0% | 0% | 0% |
| | KO | 0% | 0% | 0% | 0% | 0% |
| Δ19 | HET | 0% | 0% | 0% | 0% | 0% |
| | KO | 20% | 0% | 0% | 0% | 0% |
| Δ92 | HET | 0% | 0% | 0% | 0% | 0% |
| | KO | 0% | 0% | 0% | 0% | 0% |
| Δ17,18 | HET | 0% | 0% | 0% | 0% | 0% |
| | KO | 57% | 21% | 0% | 0% | 100% |
| Δ17,18,92 | HET | 0% | 0% | 0% | 0% | 0% |
| | KO | 100% | 100% | 0% | 100% | 100% |

Supplementary Table 2

**Summary of skeletal malformations in miR-17~92 mutant mice.**

(a) Between 4$^{th}$ and 5$^{th}$ digits; n>5 mice

| | *miR-17~92* | | | | | |
|---|---|---|---|---|---|---|
| **Vertebral transformation** | **wt** | | **het** | | **ko** | |
| **V14 (T7 to T8)** | 0/18 | **(0%)** | 0/26 | **(0%)** | 10/10 | **(100%)** |
| **V20 (T13 to L1a)** | 0/18 | **(0%)** | 0/26 | **(0%)** | 10/10 | **(100%)** |
| **V26 (L6 to S1)** | 1/18 | **(6%)** | 12/26 | **(46%)** | 10/10 | **(100%)** |

Supplementary Table 3

**Homeotic transformations in *miR-17~92*$^{\Delta}$ animals.**

T13 to L1a indicates the transformation of the 13$^{th}$ thoracic vertebra to a vertebra with rudimental or no ribs; T, thoracic vertebrae; L, lumbar vertebrae; S, sacral vertebrae.

| | *miR-17~92 Allelic Series* | | | | | | | | | | | |
|---|---|---|---|---|---|---|---|---|---|---|---|---|
| **Vertebral transformation** | **all wt** | | **Δ17** | | **Δ18** | | **Δ19** | | **Δ92** | | **Δ17,18** | **Δ17,18,92** |
| **V14 (T7 to T8)** | 0/97 | **(0%)** | 5/9 | **(56%)** | 0/9 | **(0%)** | 0/9 | **(0%)** | 0/9 | **(0%)** | 7/7 **(100%)** | 4/4 **(100%)** |
| **V20 (T13 to L1a)** | 0/97 | **(0%)** | 7/9 | **(78%)** | 0/9 | **(0%)** | 0/9 | **(0%)** | 0/9 | **(0%)** | 7/7 **(100%)** | 4/4 **(100%)** |
| **V26 (L6 to S1)** | 10/97 | **(10%)** | 9/9 | **(100%)** | 0/9 | **(0%)** | 0/9 | **(0%)** | 1/9 | **(11%)** | 7/7 **(100%)** | 4/4 **(100%)** |

Supplementary Table 4

**Homeotic transformations in mice from the miR-17~92 allelic series.**

T13 to L1a indicates the transformation of the 13$^{th}$ thoracic vertebra to a vertebra with rudimental or no ribs; T, thoracic vertebrae; L, lumbar vertebrae; S, sacral vertebrae.

Supplementary Note

**Reduction of miR-18 expression in miR-17~92$_{\Delta 17/\Delta 17}$ mice.**

RT-qPCR and small RNA-seq experiments to wild type and homozygous mutant mice from the *miR-17~92* allelic series revealed that deletion of the components of the miR-17 family is accompanied by a concomitant reduction of the expression of miR-18a (Fig. 1d and Supplementary Fig. 1). However, our analysis of the RNA-seq data described in Fig. 6 and Supplementary Fig. 6 suggests that this reduction has very limited, if any, functional consequences. In particular, we found that in *miR- 17~92*$_{\Delta 17,18/\Delta 17,18}$ embryos many more genes are de-regulated compared to *miR- 17~92*$_{\Delta 17/\Delta 17}$ mice. This shows that the expression of miR-18a in *miR-17~92*$_{\Delta 17/\Delta 17}$ mice, albeit lower than in wild-type animals, is sufficient to repress miR-18a targets. This, combined with the interesting observation that even complete miR-18a ablation (as in *miR-17~92*$_{\Delta 18/\Delta 18}$ mice) leads to de-regulation of only a handful of genes, suggests that miR-18a plays a largely ancillary role to miR-17.